Journal of Solar Energy Research (JSER)

Journal homepage: www.jser.ut.ac.ir

Optimal Allocation of Renewable Sources with Battery and Capacitors in Radial Feeders for Reliable Power Supply Using Pathfinder Algorithm

D Sreenivasulu Reddy[a], Varaprasad Janamala[b*]

[a&b]*Department of Electrical and Electronics Engineering, School of Engineering and Technology, CHRIST (Deemed to be University), Bangalore-560074, Karnataka, India.*

ARTICLE INFO

Article Type:

Research Article

Received:10.05.2023
Accepted:07.12.2023

Keywords:
Renewable energy
Energy storage system
Islanding mode
Distribution network
Pathfinder algorithm
Multi-objective optimization

A B S T R A C T

Allocating renewable energy systems (RESs) in an electrical distribution system (EDS) is crucial to achieving various objectives. However, their intermittency presents several challenges. In this connection, an efficient meta-heuristic pathfinder algorithm (PFA) is employed to determine the optimal location and size of photovoltaic (PV) and wind turbine (WT) systems, along with energy storage systems (ESS) and capacitor banks (CB) for both grid and islanding modes of operations. An objective function was formulated for loss reduction, greenhouse gas (GHG) emissions, and voltage profile improvement. The simulation results for the IEEE 33-bus EDS system are shown for two cases: grid-connected and islanding. The computational effectiveness of the PFA was compared with that reported in the literature. The PFA results showed an outstanding ability to resolve difficult optimisation problems. In addition, the optimal size of the RES when the network operates in the grid-connected mode can significantly improve the performance. The real power losses and GHG emissions were reduced by 48.49 % and 67.75% with PV systems and the other, respectively, whereas WT systems they are reduced to 69.68 % and 67.85 %, respectively. However, a combination of ESS, CB, and PV/WT can render the EDN sustainable for the islanding mode of operations.

1. Introduction

Many power systems worldwide have encountered instances of blackouts owing to the imbalance between power generation and load, as discussed by Alhelou et al. [1]. Notable examples include India in 2012 and 2001, Indonesia in 2005, Southern Brazil in 1999, Brazil and Paraguay in

*Corresponding Author Email: varaprasad.janamala@christuniversity.in

Cite this article: Sreenivasulu Reddy, D., & Janamala, V. (2023). Optimal Allocation of Renewable Sources with Battery and Capacitors in Radial Feeders for Reliable Power Supply Using Pathfinder Algorithm. Journal of Solar Energy Research, 8(4), 1651-1662. doi: 10.22059/jser.2023.358718.1299

DOI: 10.22059/jser.2023.358718.1299 DOR: 20.1001.1.25883097.2023.8.4.1.3

2009, Italy in 2003, the Northeast US and Canada in 2003, and Pakistan in 2023. To mitigate the occurrence of such blackouts, it is imperative to integrate the generation resources, reactive power compensation devices, load shedding (LS), and demand response (DR), as highlighted by Li et al. [2].

Conversely, remarkable progress has been made in incorporating renewable energy (RE) sources and emerging electric vehicles (EVs) to combat global warming and pollution, as emphasised by Streimikiene et al. [3]. However, despite their environmental advantages, these technologies present challenges in operating and controlling power systems owing to their unpredictable and stochastic behaviour, as discussed by Das et al. [4]. To mitigate these potential consequences, it is essential to integrate RE sources into electrical distribution systems (EDSs) in an effective manner.

In this regard, Ghaffarzadeh et al. [5] proposed a methodology to identify optimal sites for solar PV plants to enhance energy efficiency by reducing losses and improving voltage profiles. Aryan Nezhad et al. [6] establish the optimal distribution of wind-turbine-based hybrid power plants, taking into account long-term fluctuations in wind speed. Hassan et al. [7] propose the modified sine cosine algorithm (MSCA) to integrate various DG technologies and enhance EDS performance, considering penetration levels and power factor limits. Khasanov et al. [8] present artificial ecosystem-based optimization-opposition-based learning (AEO-OBL), an improved approach for maximizing the benefits of DG unit allocation in EDSs. This method incorporates stochastic renewable DG units and evaluates suitable buses for DG integration using the loss sensitivity index (LSI). Selim et al. [9] presented a hybrid optimisation strategy that combines the loss sensitivity factor, analytical methods, and sine-cosine algorithm (SCA) to determine the optimal DG allocation in EDSs. Ali et al. [10] utilize the improved wild horse optimization (IWHO) algorithm to determine the ideal location and size of DGs, aiming to reduce operational losses, improve the voltage profile, and enhance reliability.

The stochastic nature of optimal DG allocation poses a significant challenge for the system operators. To address this issue, energy storage systems (ESS) have gained widespread recognition as a means to mitigate the adverse impacts of renewable energy sources (REs) and electric vehicles (EVs) as well as to counterbalance energy imbalances resulting from generator or load failures or fluctuations. McIlwaine et al. [11], ESSs are employed on the generation side to reduce prediction inaccuracies, investment and operational costs, and curtailment renewable energy. Network operators (NO) utilise ESSs for energy arbitrage, minimise production costs, manage operating reserves, address ramping issues, optimise network replacement, deferral/expansion planning, and other applications aimed at reducing costs. On the distribution side, ESSs find utility in backup power, peak-shaving, and energy auctions. Consequently, ESSs have emerged as a distinct approach for addressing the various uncertainties prevalent in modern power systems.

Numerous researchers have attempted to determine the optimal allocation of RE-based distribution generation (DG) and ESSs in electrical distribution networks (EDNs) to enhance energy efficiency irrespective of the level of uncertainty involved, as discussed by Worku et al. [12]. The optimal allocation of ESSs is regarded as a complex, nonlinear optimisation problem that necessitates the use of effective metaheuristic algorithms. This is primarily because of the need for a solution that considers multiple objectives, multiple constraints, and various types of variables, as emphasised by Venkateswaran et al. [13].

Das et al. [14] employed a model where the energy storage system (ESS) was represented as a PQ injection source with a variable power factor. This model was optimally integrated into a medium-voltage electrical distribution network (EDN) along with solar and wind systems. The objective was to enhance the performance and power quality of the network. Zheng et al. [15] utilized the voltage violation risk index to guide the search for optimal locations, and subsequently employed the natural aggregation algorithm (NAA) to determine the optimal sizes and locations. The main objectives of their study were focused on economic benefits while mitigating voltage fluctuations caused by renewable energy (RE) variability. Lei et al. [16] employed a hybrid multi-objective particle swarm optimization-genetic algorithm (PSO-GA) approach to solve for the optimal location and sizing of a vanadium redox flow battery (VRB)-based ESS in wind turbine (WT) energy storage systems. Their objectives included load curtailment reduction, greenhouse gas emissions, distribution loss, and investment costs. Al-Ghussain et al. [17] conducted a techno-economic analysis of photovoltaic (PV) and wind turbine (WT) systems with various types of ESSs. The multi-objective optimisation problem was solved using the generalised reduced gradient

(GRG) algorithm. Kiptoo et al. [18] presented a mixed-integer linear programming (MILP) algorithm-based study for isolated RE-integrated microgrid (MG) planning. This study incorporated demand response and ESS costs. Salman et al. [19] aimed to minimize the total cost while solving for the ESS in grid-connected and islanded MG operations. They utilised linear and nonlinear programming along with GAMS software. Javed et al. [20] conducted an economic analysis of batteries, pumped hydro, and their combination with PV and WT systems for stand-alone applications. The multi-objective function is solved using the PSO algorithm. Xie et al. [21] proposed an MILP approach to optimize the ESS, considering a reduction in the total operating cost. This study incorporated the formulation of battery energy exchange (BEE) as a virtual storage for demand response (DR). Memon et al. [22] presented a comparative study of the GRG algorithm and HOMER software for the design of a standalone hybrid microgrid (MG) (with solar, wind, and ESS) for remote areas and grid applications. This study considered social and environmental benefits. Janamala et al. [23] employed the coyote optimization algorithm (COA) to design a flexible photovoltaic system with an ESS for stand-alone operation, considering variable electric vehicle (EV) load penetration. The integration of capacitor banks (CBs) into electrical distribution networks (EDN) has been shown to improve the voltage profile, reduce distribution losses, and enhance voltage stability. Various metaheuristic approaches have been explored to optimise the allocation of CBs in EDNs for mitigating the impact of EV load penetration Janamala [24]. Giridhar et al. [25] proposed the Mayfly algorithm (MA) for optimizing an ESS integrated with a distribution-static synchronous compensator (DSTATCOM) in a photovoltaic distribution network, aiming to reduce real power losses. Inkollu et al. [26] introduced the hunter-prey optimization (HPO) algorithm to solve for multiple PV systems in EDNs, considering multiple objective functions such as loss, voltage profile, maximization of PV penetration, and reduction of greenhouse gas (GHG) emissions. Aryan Nezhad et al. [27] proposed a hybrid RE system comprising PV, WT, and ESS to address uncertainties in PV and WT generation due to weather conditions. Khasanov et al. [28] employed the rider optimisation algorithm (ROA) to determine the optimal sizes and locations of WT, PV, and biomass-based DGs in the EDN with ESS. The primary goal is to minimise the overall power and energy losses.

These studies provide evidence for the significant role of energy storage systems (ESS) in renewable energy-integrated microgrids (MG) and the dynamic nature of electric vehicle (EV) load changes. Furthermore, the design of an ESS is of utmost importance in remote, islanded, and grid-connected modes of operation, as it affects technical performance, reliability, and economic considerations. However, the optimisation problem poses a challenge owing to the presence of multiple objectives, numerous variables, and various constraints. Although the literature presents several heuristic techniques, it is important to note that not all algorithms are suitable for all types of optimisation problems, as highlighted by the no-free-lunch (NFL) theorem Adam et al. [29], which emphasises the limitations of local or premature convergence. Hence, researchers are driven to develop new, simplified, and efficient algorithms or to enhance the convergence properties of existing algorithms through modifications or hybridisation, as noted by Kumar et al. [30].

Recently, the pathfinder algorithm (PFA) has emerged as a promising approach that mimics the movement of a group of animals with a leader directing the path, as demonstrated by Yapici et al. [31]. PFA can be effectively employed to explore and exploit resources, resembling hunting and food supply behaviours observed in nature. By following the leader and collaborating with neighbouring individuals, various agents can collectively investigate and exploit targets in the search space, as discussed by Janamala [32].

In contrast to these studies, this study makes several significant contributions. First, it determines the optimal placement and sizing of renewable energy systems (such as photovoltaic or wind turbines) in conjunction with energy storage systems (ESS) for both grid and islanding applications. Moreover, the computational efficiency of the pathfinder algorithm (PFA) is compared to other meta-heuristic techniques. Second, the study presents simulation results conducted on an IEEE 33-bus radial electrical distribution network (EDN) for various scenarios. These scenarios include different configurations of one, two, and three locations along with their corresponding sizes. For each scenario, both the grid-connected and islanding modes were considered, resulting in a comprehensive analysis. Finally, the outcomes obtained by applying the pathfinder algorithm demonstrated its superior capability in addressing complex optimisation problems.

Section 2 describes the mathematical modelling of the components within the electrical distribution network. Section 3 introduces the multi-objective problem, while Section 4 presents a concise mathematical model of the pathfinder algorithm. The simulation findings are discussed in section 5, and the paper concludes with the key insights presented in section 6.

2. Modeling of Renewable Distribution Network

This section provides the mathematical modeling of the different components employed in the EDN in connection with the optimization variables.

2.1. Photovoltaic System

PV systems provide active power to the grid via a DC/AC inverter with a power factor of unity. The required components in PV systems considering the grid and islanding modes of operation are shown in Figure 1 and 2, respectively.

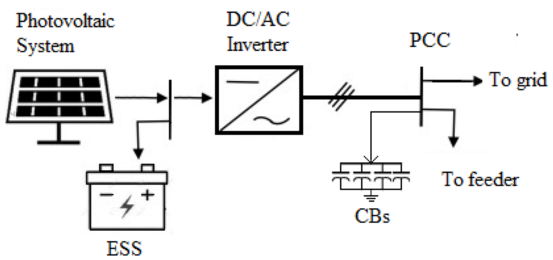

Figure 1. Schematic diagram of grid-connected feeder with PV, ESS and CBs

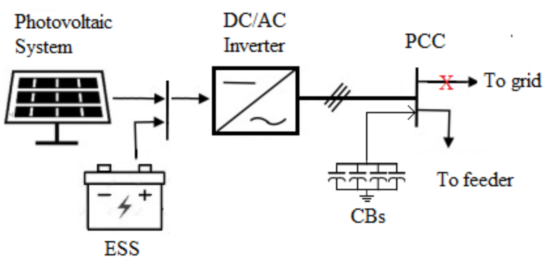

Figure 2. Schematic diagram of islanded feeder with PV, ESS and CBs

In grid-connected mode, the ESS and CBs are treated only as storage. In the islanding mode, both ESS and CBs were considered in the discharging mode to satisfy the feeder load. In the grid-connected mode, the net power injections at bus k are determined by subtracting the PV and ESS injections from the base case load, and are given by Janamala et al. [23].

$$P_{d(k)} = P_{d,0(k)} - \left(P_{pv(k)} - P_{ess(k)}\right) \quad (1)$$

$$Q_{d(k)} = Q_{d,0(k)} - \left(Q_{pv(k)} - Q_{ess(k)}\right) \quad (2)$$

In the islanded mode, the net power injections at bus k are given by Giridhar et al. [25],

$$P_{d(k)} = P_{d,0(k)} - \left(P_{pv(k)} + P_{ess(k)}\right) \quad (3)$$

$$Q_{d(k)} = Q_{d,0(k)} - \left(Q_{pv(k)} + Q_{ess(k)}\right) \quad (4)$$

2.2. Wind Turbine System

The WT system provides active and reactive power to the grid via an AC/AC converter at a variable power factor Hassan et al. [7]. The required components in the WT systems for the grid-connected and islanding modes are shown in Figure 3 and 4, respectively.

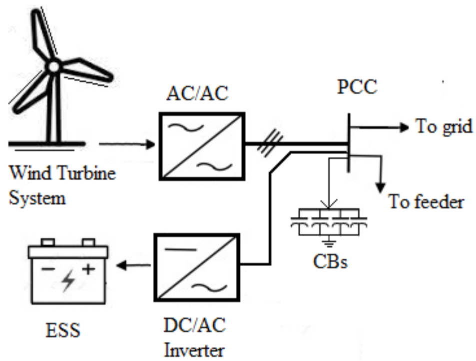

Figure 3. Schematic diagram of grid-connected feeder with WT, ESS and CBs

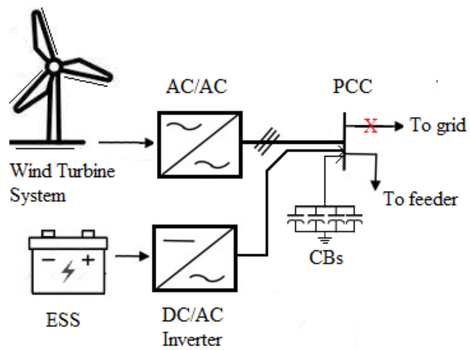

Figure 4. Schematic diagram of islanded feeder with

WT, ESS and CBs

In the grid-connected mode, the net power injections at bus-*k* are given by Hassan et al. [7],

$$P_{d(k)} = P_{d,0(k)} - \left(P_{wt(k)} - P_{ess(k)}\right) \quad (5)$$

$$Q_{d(k)} = Q_{d,0(k)} - \left(Q_{wt(k)} + Q_{cb(k)} - Q_{ess(k)}\right) \quad (6)$$

In the islanded mode, the net power injections at bus-*k* are given by Hassan et al. [7],

$$P_{d(k)} = P_{d,0(k)} - \left(P_{wt(k)} + P_{ess(k)}\right) \quad (7)$$

$$Q_{d(k)} = Q_{d,0(k)} - \left(Q_{wt(k)} + Q_{cb(k)} + Q_{ess(k)}\right) \quad (8)$$

3. Problem Formulation

This section describes the proposed multi-objective function with planning and operational constraints while integrating ESS in EDN embedded with PV/WT systems.

3.1. Multi-Objective Function

Several key factors were considered to develop the multi-objective function. First, the reduction in distribution losses, as highlighted by Hassan et al. [7], was prioritized. Minimizing greenhouse gas (GHG) emissions, as emphasized by Inkollu et al. [26], is also a significant objective. Additionally, improving the voltage profile, as discussed by Janamala et al. [23], is deemed crucial. These objectives were mathematically formulated to create a comprehensive multi-objective function that captured the essence of these considerations. The specific mathematical representation of the multi-objective function is as follows:

$$P_{loss} = \sum_{l=1}^{nl} I_l^2 r_l \quad (9)$$

$$AVDI = \frac{1}{nb}\sum_{n=1}^{nb}\left(1 - V_n\right) \quad (10)$$

$$GHG_e = \left(k_c + k_n + k_s\right)\left(P_{loss} + \sum_{k=1}^{nb} P_{d(k)}\right) \quad (11)$$

$$OF = \min\left(P_{loss} + AVDI + GHG_e\right) \quad (12)$$

3.2. Planning and Operational Constraints

In this study, a single PV/WT system with sufficient ESS was proposed for the optimisation of any EDNs. Thus, the number of PV/WT locations and their corresponding sizes are the major search variables. In addition, the power factor is another search variable that optimises the WT parameters.

However, the voltage magnitudes of all buses should be maintained within specified limits, the size of the PV/WT system should not exceed the total active and reactive power demands of the network, and the sum of the PV/WT and ESS capacity should be equal to the real and reactive power loads and losses at any time. This study has considered the following constraints as defined by Inkollu et al. [26],

$$V_{\min} \le V_n \le V_{\max} \quad (13)$$

$$P_{pv} < \sum_{k=1}^{nb} P_{d(k)} \quad (14)$$

$$P_{pv} + P_{ess} = P_{loss} + \sum_{k=1}^{nb} P_{d(k)} \quad (15)$$

$$Q_{cb} + Q_{ess} = Q_{loss} + \sum_{k=1}^{nb} Q_{d(k)} \quad (16)$$

$$P_{wt} < \sum_{k=1}^{nb} P_{d(k)} \quad (17)$$

$$P_{wt} + P_{ess} = P_{loss} + \sum_{k=1}^{nb} P_{d(k)} \quad (18)$$

$$Q_{wt} + Q_{cb} + Q_{ess} = Q_{loss} + \sum_{k=1}^{nb} Q_{d(k)} \quad (19)$$

To ensure successful resolution of the optimisation problem, it is essential to satisfy specific equations for different scenarios. When solving with photovoltaic (PV) systems alone, it is crucial to satisfy Eq. (13) and Eqs. (14) to (16). However, if wind turbine (WT) systems are considered in isolation, Eq. (13) and Eqs. (17) to (19) must be satisfied: These equations play a vital role in ensuring the accuracy and validity of the optimisation process, tailored to the specific characteristics and requirements of each renewable energy system.

4. Solution Methodology

In this section, the pathfinder algorithm (PFA) proposed by Yapici et al. [31] is proposed for solving the multi-objective optimization problem, and the steps involved in the process are explained mathematically.

4.1. Pathfinder Algorithm

PFA uses the features and survival tactics of animal groups. It divides group animals into leaders and followers, based on their fitness values. The leader must find the best food and mark it for the followers. Followers follow the pathfinder's markers and the sense of direction. When the number of algorithm iterations increases, the two forms of task become interchangeable according to the individual's search capacity. In other words, the pathfinders may become followers. Similarly, followers can be potential pathfinders. By utilizing the specific foraging behaviors of any group of animals, mathematical modeling of PFA can be explained as follows.

Exploration phase: In this phase, the pathfinder changes its location using the following update formula defined by Yapici et al. [31]:

$$x_{j(i+1)} = x_{j(i)} + 2r_1\left[x_{j(i)} - x_{j(i-1)}\right] + P \tag{20}$$

Exploitation phase: In this phase, the follower changes its location by using the following update formula defined by Yapici et al. [31]:

$$\begin{aligned} x_{j(i+1)} = x_{j(i)} + \rho r_2\left[x_{k(i)} - x_{j(i)}\right] + \\ \beta r_3\left[x_{l(i)} - x_{j(i)}\right] + \delta,\ j \geq 2 \end{aligned} \tag{21}$$

The following two expressions were used to define δ and *P*, defined by Yapici et al. [31].

$$\delta = \left(1 - \frac{i}{i_{\max}}\right) r_4 d_{jk},\ d_{jk} = \left\| x_{k(i)} - x_{j(i)} \right\| \tag{22}$$

$$P = r_5 e^{\lambda},\ \lambda = \frac{-2i}{i_{\max}} \tag{23}$$

By tuning δ and P in every iteration, PFA reaches the global optima. Upon reaching the maximum number of iterations, PFA terminates the iterative procedure and provides global optima and its solution vector. Detailed information on PFA can be obtained from Yapici et al. et al. [31].

4.2. Steps for Solving the Proposed Problem

The major steps of this study are as follows:

St 1: Read the test system data and define the mode of operation (i.e. grid-connected or islanding mode).

St 2: For the grid-connected mode, the best location and sizes of PV or WTs for peak loading conditions were determined by optimising the proposed objective function and constraints.

St 3: For the islanding mode, the best location and sizes of CBs and ESSs are determined considering the day-long load profile PV/WT generation profiles.

St 4: Compare the results with literature works.

5. Simulation Results

Simulations were performed on an IEEE 33-bus, and simulations were conducted on a test system, as described by Dolatabadi et al. [33], using MATLAB R2023b software on a PC with 4 GB of RAM, a 64-bit operating system, and an Intel® CoreTM i5-2410M CPU running at a clock speed of 2.30 GHz. The performance of the electrical distribution system (EDS) was evaluated using the MATPOWER software-based Newton-Raphson (NR) load flow method, as developed by Zimmerman et al. [34]. The grid-connected mode was examined in the initial stage of the simulations. The proposed algorithm was employed to determine the optimal placement and size of photovoltaic (PV) or wind turbine (WT) systems, in addition to the required capacitor banks (CBs), specifically tailored for peak load conditions. The utilisation of the proposed algorithm facilitated the identification of the most efficient location and size of the PV/WT system, along with the necessary CBs, with the aim of optimising the overall performance of the grid-connected mode.

5.1. Grid-Connected Mode

Case 1: In this case, the test system was assumed to be working healthy in the grid-connected mode without any RE-based DGs, ESSs, or CBs. Furthermore, the total load and distribution losses are assumed to be supplied by the grid alone. The test system had peak loading conditions of 3715 kW and 2300 kV Ar. The operating voltage was 12.66 kV. By performing load flow, the network has exposed to a total real and reactive power losses of 202.3 kW, and 134.9 kVAr, respectively. The minimum voltage magnitude in the network was observed at bus-18 at 0.9132 p.u., and the overall

AVDI and total GHG emissions were estimated to be 0.0312 and 7851.6 lb/h, respectively.

Case 2: In this case, the burden on the grid should be reduced by optimally integrating the PV system. The optimal location and size of a single PV system were determined using the PFA. At bus-6, the optimal capacity of the PV system was determined as 2582 kW. By this, the network real and reactive power losses are reduced to 103.4 kW, and 74.5 kVAr, respectively. The minimum voltage magnitude in the network was increased to 0.9515 p.u. at bus-18 and the AVDI was reduced to 0.0248. In addition, GHG emissions were reduced to 2531.9 lb/h, respectively.

Case 3: This case solves for optimal allocation of the WT system. The optimal location and size of the single WT system were determined using PFA. At bus-6, the optimal capacity of the WT system was determined as 2543.6 kW with an optimal operating power factor of 0.8243. By this, the network real and reactive power losses are reduced to 61.34 kW, and 48.35 kVAr, respectively. The minimum voltage magnitude in the network was increased to 0.9668 p.u. at bus-18 and the AVDI was reduced to 0.0144. In addition, GHG emissions were reduced to 2524.2 lb/h, respectively..

Figure 5 shows a comparison of the three goal functions in terms of Base Case 1. PV systems minimised real power losses by 48.88%, AVDI by 20.51%, and GHG emissions by 67.75%. In comparison, the WT system reduced these values by 69.68%, 53.85%, and 67.85%, respectively. As a result of their combined active and reactive power injections in the network, WT systems contribute more to boosting EDS performance, specifically distribution loss and AVDI. As proved by Janamala [24], reactive power compensation also plays an important role in improving the EDS performance. GHG emission reductions, however, are nearly the same because both penetrate the same amount of real power in the network.

In addition to the aforementioned simulations, further analyses were conducted utilizing the coyote optimization algorithm (COA) by Pierezan et al. [35], and Mayfly algorithm (MA) by Zervoudakis et al. and hunter prey optimization (HPO) by Naruei et al. [37], was also employed in the simulations. These algorithms were selected based on their effectiveness and suitability for the optimisation problem at hand, further enhancing the comprehensiveness of this study. The results are presented in Table 2. Almost all algorithms resulted in the same best location and optimal size, as determined by the proposed PFA. On the other side, the repetitive simulations of 50 independent runs are also compared in terms of worst, median and std. for objective function 1. The lower values of these quantities indicate the superiority of PFA over the other algorithms.

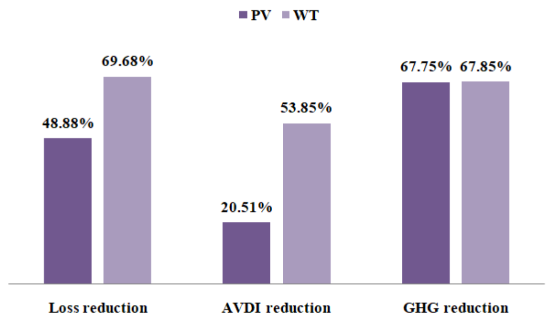

Figure 5. Comparison of objective functions

5.2. Islanding Mode

In this scenario, the network is assumed to have hourly variations, as described by Nguyen et al.[38], for the load profile, PV, and WT, as shown in Figure 6.

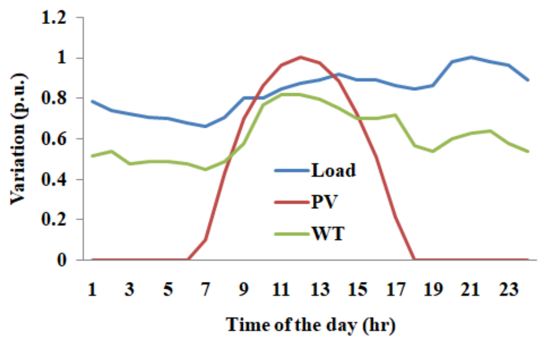

Figure 6. Variation in network load, PV and WT generations

Case 1: Assuming that the network is in the islanding mode, load flow is carried out by treating the PV/WT site as a slack bus. First, it was assumed that the network had no PV or WT system. Consequently, the required energy of the network must be supplied only by the ESS and the CBs. Thus, the energy required for 24 h was 74752 kWh/ day. In addition, the required reactive power was estimated to be 46499 kVAr/ day. In this case, the energy loss distribution is approximately 1481.05 kWh, or 1.98%. Because there are no other sources in the network, the same number of ESS and CBs is required to sustain the network in the islanding mode. The average power losses per hr are 61.71 kW and 47.356 kVAr, respectively. The minimum average voltage at bus-25 was determined to be 0.9711 p.u. and the AVDI was 0.0005. The total and average GHG emissions were estimated to be 153067 lb/day and 6377.78 lb/h, respectively.

Table 1. Network performance with PV system

Parameter	**Base**	**COA**	**MA**	**HPO**	**PFA**
PV (kW)	–	2581.919	2581.902	2581.905	2581.886
Location #	–	6	6	6	6
P_{loss} (kW)	202.293	103.405	103.405	103.405	103.405
Q_{loss} (kVAr)	134.896	74.479	74.479	74.479	74.479
V_{min} (p.u.)	0.913	0.952	0.952	0.952	0.952
AVDI	0.031	0.025	0.025	0.025	0.025
GHG (lb/h)	7851.6	2531.9	2531.9	2531.9	2531.9
Worst	–	105.22	104.801	104.241	104.284
Median	–	103.935	103.424	103.523	103.41
Std.	–	0.534	0.409	0.225	0.316
Avg. Time (sec)	–	12.064	12.052	12.022	11.574

Table 2. Network performance with WT system

Parameter	**Base**	**COA**	**MA**	**HPO**	**PFA**
WT (kW)	–	2543.5	2543.5	2543.5	2543.7
Power factor	–	0.824	0.824	0.824	0.824
Location #	–	6	6	6	6
P_{loss} (kW)	202.293	61.34	61.34	61.34	61.34
Q_{loss} (kVAr)	134.896	48.349	48.349	48.349	48.35
V_{min} (p.u.)	0.913	0.967	0.967	0.967	0.967
AVDI	0.031	0.014	0.014	0.014	0.014
GHG (lb/h)	7851.6	2524.4	2524.4	2524.4	2524
Worst	–	69.173	68.593	67.577	67.036
Median	–	62.459	62.565	62.597	62.129
Std.	–	1.453	1.461	1.453	1.043
Avg. Time (sec)	–	2543.5	2543.5	2543.5	2543.7

Table 3. Optimal design of ESS for islanding conditions

	ESS (kWh/ day)	**CB (kVAr/ day)**	**P_{loss} (kWh/ day)**	**GHG (lb/day)**	**ESS Capacity (kW)**	**CB Capacity (kVAr)**
Case 1	74752	46499	1481.05	153067	3805.625	2369.536
Case 2	55801	46499	1481.05	114261	3805.625	2369.536
Case 3	37361	20818	1481.05	76503	2203.157	1268.914

The required maximum capacities of the ESS and CB unit sizes at bus-6 were estimated at 3805.625 kW and 2369.536 kVAr, respectively.

Case 2: In this case, the network was assumed to have only the PV system, as determined in the grid-connected mode. Thus, the required energy in the network needs to be supplied only by the ESS by excluding the PV generation and the required reactive power supply by only the CBs. The energy required for 24 h was 55801 kWh/ day. In addition, the required reactive power was estimated to be 46499 kVAr/ day. In this case, the energy loss distribution is approximately 1481.05 kWh, or 2.65%. Because there are no other reactive power sources in the network, the same amount of CBs is required to sustain the network in the islanding mode. The total and average GHG emissions were estimated at 114261.2 lb/day and 4760.833 lb/h, respectively. In comparison to Case 1, both the ESS capacity and GHG emissions were reduced by 25.35 % owing to the PV generation. The required maximum capacities of the ESS and CB unit sizes at bus-6 were estimated at 3805.625 kW and 2369.536 kVAr, respectively. These capacities are the same as in Case 1 because the PV system may not be available throughout the day, particularly during the peak time.

Case 3: In this case, the network was assumed to have only the WT system, as determined in the grid-connected mode. Thus, the required energy in the network needs to be supplied only by the ESS by excluding the WT generation and the required reactive power supply by only the CBs. The energy required for 24 h was 37361.1 kWh/ day. In addition, the required reactive power was estimated to be 20818 kVAr/ day. In this case, the energy loss distribution was approximately 1481.05 kWh, or 3.96%. Because the WT system supplies both real and reactive power in the network, the CBs size is also reduced. The total and average GHG emissions were estimated at 76502.77 lb/day and 3187.62 lb/h, respectively. In comparison to Case 1, both the ESS capacity and GHG emissions were reduced by 50 % owing to the WT generation throughout the day. The required maximum capacities of the ESS and CB unit sizes on bus-6 were estimated to be 2203.157 kW and 1268.914 kVAr, respectively.

A comparison of the case studies is presented in Table 3. The voltage profiles of the network for different scenarios are compared in Figure 7. It can be seen clearly that the voltage profile is satisfactory for the WT system.

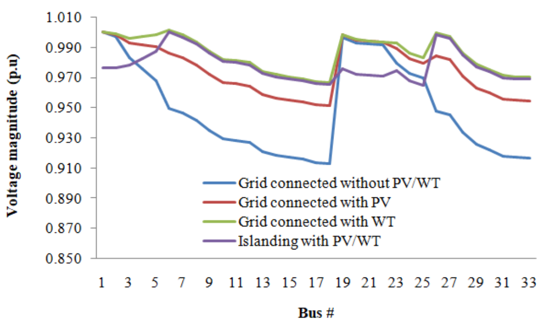

Figure 7. Comparison of voltage profile for different scenarios

6. Conclusion

A novel heuristic Pathfinder algorithm (PFA) is presented to solve the optimal allocation of RE systems in an EDN. A multi-objective function using real power loss, voltage profile, and greenhouse gas (GHG) emissions was defined and optimized using PFA. First, the location and capacities of photovoltaic (PV)/ wind turbine (WT) systems were optimally determined by considering the network in the grid-connected mode. In the second stage, the required energy storage system (ESS) and capacitor banks (CBs) were evaluated for islanding conditions, considering hourly variations in the load profile and PV/WT generation. Simulations were performed using an IEEE 33-bus test system. In addition, the network performance was significantly improved with WTs than with PV systems. In addition, the capacitors of the ESS and CBs drastically decreased with WTs compared to PVs. In addition, COA, MA, and HPO were used to compare the PFA performance. Based on 50 independent simulations of each case using each algorithm, a statistical analysis was performed. The lower values of these quantities indicate the superiority of the PFA over the compared algorithms.

Although the results show an overall improvement in EDS performance with either PV or WT alone, there is a need for hybridization of both sources to provide high reliability and minimize the capacities of the ESSs. Furthermore, although PFA has demonstrated promising answers to complicated optimization issues, any heuristic technique tends to trap local optima. To avoid this, either exploration or exploitation must be improved, or algorithm hybridization is required. These two issues were not addressed in this study; however, they can be considered future research directions.

Nomenclature

$P_{d(k)}$	Net active power loadings of bus-*k* after PV/WT integration
$Q_{d(k)}$	Net reactive power loadings of bus-*k* after PV/WT integration
$P_{d,0(k)}$	Net active power loadings of bus-*k* before PV/WT integration
$Q_{d,0(k)}$	Net reactive power loadings of bus-*k* before PV/WT integration
$P_{pv(k)}$	Active injection by PV system at bus-*k*
$Q_{cb(k)}$	Reactive power injection by CBs at bus-*k*
$P_{wt(k)}$	Active power injections by WT system at bus-*k*
$Q_{wt(k)}$	Reactive power injections by WT system at bus-*k*
$P_{ess(k)}$	Active power support by ESS at bus-*k*
$Q_{ess(k)}$	Reactive power support by ESS at bus-*k*
P_{loss}	Distribution real power losses
Q_{loss}	Distribution reactive power losses
AVDI	Average voltage deviation index
GHG_e	GHG emission
V_n	Voltage magnitude of bus-*n*

nb	Number of buses in the network
nl	Total braches/lines in the network
k_c	Coefficient of CO_2
k_n	Coefficient of NO_x
k_s	Coefficient of SO_2
OF	Overall objective function
$x_{j(i+1)}$	Updated Pathfinder vector in iteration *i+1*
$x_{j(i)}$	Pathfinder vector in iteration *i*
$x_{j(i-1)}$	Pathfinder vector in iteration *i-1*
r_1, r_2, r_3, r_4, r_5	Random numbers between 0 and 1
ρ	Coefficient of interaction to define movement with neighbours
β	Coefficient of attractions to ensure random distance with prey and leader
$x_{j(i)}, x_{j(i)}, x_{l(i)}$	Vectors of *j*th, *k*th and *l*th member in the search space at iteration-*i*
d_{jk}	Distance among two members in search space
i_{max}	Maximum number of iterations

References

[1] Haes Alhelou, H., Hamedani-Golshan, M. E., Njenda, T. C., & Siano, P. (2019). A survey on power system blackout and cascading events: Research motivations and challenges. Energies, 12(4), 682. DOI: 10.3390/en12040682

[2] Li, M. J., Tse, C. K., Liu, D., & Zhang, X. (2023). Cascading Failure Propagation and Mitigation Strategies in Power Systems. IEEE Systems Journal. DOI: 10.1109/JSYST.2023.3248044

[3] Streimikiene, D., Balezentis, T., Alisauskaite-Seskiene, I., Stankuniene, G., & Simanaviciene, Z. (2019). A review of willingness to pay studies for climate change mitigation in the energy sector. Energies, 12(8), 1481. DOI: 10.3390/en12081481

[4] Das, H. S., Rahman, M. M., Li, S., & Tan, C. W. (2020). Electric vehicles standards, charging infrastructure, and impact on grid integration: A technological review. Renewable and Sustainable Energy Reviews, 120, 109618. DOI: 10.1016/j.rser.2019.109618

[5] Ghaffarzadeh, N., & Faramarzi, H. (2022). Optimal Solar plant placement using holomorphic embedded power Flow Considering the clustering technique in uncertainty analysis. Journal of Solar Energy Research, 7(1), 997-1007. DOI: 10.22059/JSER.2022.330961.1221

[6] Aryan Nezhad, M. (2021). Economic Impacts of Long-Term Wind Speed Changes on Optimal Planning of a Hybrid Renewable Energy System (HRES). Journal of Solar Energy Research, 6(1), 656-663. DOI: 10.22059/JSER.2021.315440.1186

[7] Hassan, A. S., Othman, E. A., Bendary, F. M., & Ebrahim, M. A. (2020). Optimal integration of distributed generation resources in active distribution networks for techno-economic benefits. Energy Reports, 6, 3462-3471. DOI: 10.1016/j.egyr.2020.12.004

[8] Khasanov, M., Kamel, S., Halim Houssein, E., Rahmann, C., & Hashim, F. A. (2023). Optimal allocation strategy of photovoltaic-and wind turbine-based distributed generation units in radial distribution networks considering uncertainty. Neural Computing and Applications, 35(3), 2883-2908. DOI: 10.1007/s00521-022-07715-2

[9] Selim, A., Kamel, S., Mohamed, A. A., & Elattar, E. E. (2021). Optimal allocation of multiple types of distributed generations in radial distribution systems using a hybrid technique. Sustainability, 13(12), 6644. DOI: 10.3390/su13126644

[10] Ali, M. H., Kamel, S., Hassan, M. H., Tostado-Véliz, M., & Zawbaa, H. M. (2022). An improved wild horse optimization algorithm for reliability based optimal DG planning of radial distribution networks. Energy Reports, 8, 582-604. DOI: 10.1016/j.egyr.2021.12.023

[11] McIlwaine, N., Foley, A. M., Morrow, D. J., Al Kez, D., Zhang, C., Lu, X., & Best, R. J. (2021). A state-of-the-art techno-economic review of distributed and embedded energy storage for energy systems. Energy, 229, 120461. DOI: 10.1016/j.energy.2021.120461

[12] Worku, M. Y. (2022). Recent advances in energy storage systems for renewable source grid integration: a comprehensive review. Sustainability, 14(10), 5985. DOI: 10.3390/su14105985

[13] Venkateswaran, V. B., Saini, D. K., & Sharma, M. (2020). Approaches for optimal planning of energy storage units in distribution network and their impacts on system resiliency. CSEE Journal of power and energy systems, 6(4), 816-833. DOI: 10.17775/CSEEJPES.2019.01280

[14] Das, C. K., Bass, O., Mahmoud, T. S., Kothapalli, G., Mousavi, N., Habibi, D., & Masoum, M. A. (2019). Optimal allocation of distributed energy storage systems to improve

performance and power quality of distribution networks. Applied Energy, 252, 113468. DOI: 10.1016/j.apenergy.2019.113468

[15] Zheng, Y., Song, Y., Huang, A., & Hill, D. J. (2019). Hierarchical optimal allocation of battery energy storage systems for multiple services in distribution systems. IEEE Transactions on Sustainable Energy, 11(3), 1911-1921. DOI: 10.1109/TSTE.2019.2946371

[16] Lei, J., Gong, Q., Liu, J., Qiao, H., & Wang, B. (2019). Optimal allocation of a VRB energy storage system for wind power applications considering the dynamic efficiency and life of VRB in active distribution networks. IET Renewable Power Generation, 13(4), 563-571. DOI: 10.1049/iet-rpg.2018.5619

[17] Al-Ghussain, L., Samu, R., Taylan, O., & Fahrioglu, M. (2020). Sizing renewable energy systems with energy storage systems in microgrids for maximum cost-efficient utilization of renewable energy resources. Sustainable Cities and Society, 55, 102059. DOI: 10.1016/j.scs.2020.102059

[18] Kiptoo, M. K., Lotfy, M. E., Adewuyi, O. B., Conteh, A., Howlader, A. M., & Senjyu, T. (2020). Integrated approach for optimal techno-economic planning for high renewable energy-based isolated microgrid considering cost of energy storage and demand response strategies. Energy Conversion and Management, 215, 112917. DOI: 10.1016/j.enconman.2020.112917

[19] Salman, U. T., Al-Ismail, F. S., & Khalid, M. (2020). Optimal sizing of battery energy storage for grid-connected and isolated wind-penetrated microgrid. IEEE Access, 8, 91129-91138. DOI: 10.1109/ACCESS.2020.2992654

[20] Javed, M. S., Ma, T., Jurasz, J., Canales, F. A., Lin, S., Ahmed, S., & Zhang, Y. (2021). Economic analysis and optimization of a renewable energy based power supply system with different energy storages for a remote island. Renewable Energy, 164, 1376-1394. DOI: 10.1016/j.renene.2020.10.063

[21] Xie, C., Wang, D., Lai, C. S., Wu, R., Wu, X., & Lai, L. L. (2021). Optimal sizing of battery energy storage system in smart microgrid considering virtual energy storage system and high photovoltaic penetration. Journal of Cleaner Production, 281, 125308. DOI: 10.1016/j.jclepro.2020.125308

[22] Memon, S. A., Upadhyay, D. S., & Patel, R. N. (2021). Optimal configuration of solar and wind-based hybrid renewable energy system with and without energy storage including environmental and social criteria: A case study. Journal of Energy Storage, 44, 103446. DOI: 10.1016/j.est.2021.103446

[23] Janamala, V., & Reddy, D. S. (2021). Coyote optimization algorithm for optimal allocation of interline–Photovoltaic battery storage system in islanded electrical distribution network considering EV load penetration. Journal of Energy Storage, 41, 102981. DOI: 10.1016/j.est.2021.102981

[24] Janamala, V. (2022). Optimal siting of capacitors in distribution grids considering electric vehicle load growth using improved flower pollination algorithm. SJEE, 19(3), 329-349. DOI: 10.2298/SJEE2203329J

[25] Giridhar, M. S., Rani, K. R., Rani, P. S., & Janamala, V. (2022). Mayfly Algorithm for Optimal Integration of Hybrid Photovoltaic/Battery Energy Storage/D-STATCOM System for Islanding Operation. International Journal of Intelligent Engineering & Systems, 15(3), 225-232. DOI: 10.22266/ijies2022.0630.19

[26] Inkollu, S. R., Anjaneyulu, G. V., NC, K., & CH, N. K. (2022). An Application of Hunter-Prey Optimization for Maximizing Photovoltaic Hosting Capacity Along with Multi-Objective Optimization in Radial Distribution Network. International Journal of Intelligent Engineering & Systems, 15(4), 575-584. DOI: 10.22266/ijies2022.0831.52

[27] Aryan Nezhad, M. (2022). Frequency control and power balancing in a hybrid renewable energy system (HRES): Effective tuning of PI controllers in the secondary control level. Journal of Solar Energy Research, 7(1), 963-970. DOI: 10.22059/JSER.2022.330109.1219

[28] Khasanov, M., Kamel, S., Rahmann, C., Hasanien, H. M., & Al‐Durra, A. (2021). Optimal distributed generation and battery energy storage units integration in distribution systems considering power generation uncertainty. IET Generation, Transmission & Distribution, 15(24), 3400-3422. DOI: 10.1049/gtd2.12230

[29] Adam, S. P., Alexandropoulos, S. A. N., Pardalos, P. M., & Vrahatis, M. N. (2019). No free lunch theorem: A review. Approximation and optimization: Algorithms, complexity and applications, 57-82. DOI: 10.1007/978-3-030-12767-1_5

[30] Kumar, A., Nadeem, M., & Banka, H. (2023). Nature inspired optimization algorithms: a

comprehensive overview. Evolving Systems, 14(1), 141-156. DOI: 10.1007/s12530-022-09432-6

[31] Yapici, H., & Cetinkaya, N. (2019). A new meta-heuristic optimizer: Pathfinder algorithm. Applied soft computing, 78, 545-568. DOI: 10.1016/j.asoc.2019.03.012

[32] Janamala, V. (2021). A new meta-heuristic pathfinder algorithm for solving optimal allocation of solar photovoltaic system in multi-lateral distribution system for improving resilience. SN Applied Sciences, 3(1), 118. DOI: 10.1007/s42452-020-04044-8

[33] Dolatabadi, S. H., Ghorbanian, M., Siano, P., & Hatziargyriou, N. D. (2020). An enhanced IEEE 33 bus benchmark test system for distribution system studies. IEEE Transactions on Power Systems, 36(3), 2565-2572. DOI: 10.1109/TPWRS.2020.3038030

[34] Zimmerman, R. D., Murillo-Sánchez, C. E., & Thomas, R. J. (2010). MATPOWER: Steady-state operations, planning, and analysis tools for power systems research and education. IEEE Transactions on power systems, 26(1), 12-19. DOI: 10.1109/TPWRS.2010.2051168

[35] Pierezan, J., & Coelho, L. D. S. (2018, July). Coyote optimization algorithm: a new metaheuristic for global optimization problems. In 2018 IEEE congress on evolutionary computation (CEC) (pp. 1-8). IEEE. DOI: 10.1109/CEC.2018.8477769

[36] Zervoudakis, K., & Tsafarakis, S. (2020). A mayfly optimization algorithm. Computers & Industrial Engineering, 145, 106559. DOI: 10.1016/j.cie.2020.106559

[37] Naruei, I., Keynia, F., & Sabbagh Molahosseini, A. (2022). Hunter–prey optimization: Algorithm and applications. Soft Computing, 26(3), 1279-1314. DOI: 10.1007/s00500-021-06401-0

[38] Nguyen, T. T., Nguyen, T. T., Duong, L. T., & Truong, V. A. (2021). An effective method to solve the problem of electric distribution network reconfiguration considering distributed generations for energy loss reduction. Neural Computing and Applications, 33, 1625-1641. DOI: 10.1007/s00521-020-05092-2